

# Impedance analysis of squirrel-cage induction motor at high harmonics condition

Aleksandr Skamyin<sup>1</sup>, Yaroslav Shklyarskiy<sup>2</sup>, Kirill Lobko<sup>2</sup>, Vasiliy Dobush<sup>2</sup>, Tole Sutikno<sup>3</sup>,  
Mohd Hatta Jopri<sup>4</sup>

<sup>1</sup>Department of Electric Power and Electromechanics, Saint Petersburg Mining University, Saint Petersburg, Russia

<sup>2</sup>Department of General Electrical Engineering, Saint-Petersburg Mining University, Saint Petersburg, Russia

<sup>3</sup>Department of Electrical Engineering, Universitas Ahmad Dahlan, Yogyakarta, Indonesia

<sup>4</sup>Faculty of Electrical and Electronic Engineering Technology, Universiti Teknikal Malaysia Melaka, Melaka, Malaysia

## Article Info

### Article history:

Received Jul 26, 2023

Revised Oct 16, 2023

Accepted Oct 21, 2023

### Keywords:

Asynchronous motor

Equivalent circuit

High harmonics

Impedance analysis

Power quality

## ABSTRACT

This study examines different methodologies for representing an asynchronous motor at higher harmonics by utilizing its equivalent circuit. Several approaches were compared based on simulation modeling. An experimental investigation was conducted in a laboratory setting using asynchronous electric motors with power ratings of 1.5 kW and 5.5 kW. The purpose of this investigation was to examine the characteristics of impedance in the presence of high-harmonic conditions. The generation of higher harmonics was achieved through the utilization of a precisely regulated thyristor rectifier in conjunction with a thyristor power controller. The findings indicate that the load on the shaft solely impacts the resistance at the fundamental harmonic, while the resistance at higher harmonics remains unaffected by the operating mode of the asynchronous motor (AM).

*This is an open access article under the [CC BY-SA](https://creativecommons.org/licenses/by-sa/4.0/) license.*



## Corresponding Author:

Mohd Hatta Jopri

Faculty of Electrical and Electronic Engineering Technology, Universiti Teknikal Malaysia Melaka

Melaka, Malaysia

Email: hatta@utem.edu.my

## 1. INTRODUCTION

The prevalence of semiconductor-based components, such as power rectifiers and inverters in electrical drives [1]–[3], as well as in renewable energy sources like photovoltaics (PVs) [4]–[6] and wind generators [7]–[9], has led to the occurrence of higher harmonic currents in power grids. Consequently, the passage of these electrical currents through the various components of the network, such as transmission lines and transformers, results in a degradation of voltage quality experienced by the end consumer. In order to enhance the quality of electricity, a range of filter-compensating devices are employed. Passive filters [10]–[12] refer to a type of electronic circuit that is designed to selectively attenuate or suppress certain frequencies in a signal without requiring. Active filters, as discussed in references [13]–[15], and hybrid filters, as mentioned in references [16]–[18], are two types of filters commonly used in various applications. To effectively choose and configure devices for the purpose of mitigating harmonics, it is imperative to possess knowledge regarding the harmonic currents present in the various branches, as well as the voltage distortion observed at the nodes. There exist numerous methodologies for the analysis of higher harmonics within power grid systems. The literature contains various methods for network analysis, which include the construction of amplitude-frequency characteristics [19]–[21]. C.I.G.R.E [20] provides recommendations regarding the utilization of methods in the domains of frequency, time, and their combination. The direct harmonic analysis method involves computing a grid for the desired frequencies. However, a significant challenge arises in

accurately representing each element of the grid at a specific frequency [22]–[24]. Numerous scholarly articles and monographs have been dedicated to the exploration of this subject [25], [26]. Furthermore, the investigation of the impedance characteristics of grid components is of significance in light of the escalating demand for power [27]–[29] and the consequent adoption of renewable energy sources [30]–[32] driven by environmental considerations and the global endeavor to mitigate greenhouse gas emissions [33]–[35]. An asynchronous alternating current (AC) motor is considered to be one of the primary electrical loads in industrial enterprises. This paper aims to analyze the current equivalent circuits of an asynchronous motor, investigate the amplitude-frequency characteristic of the motor impedance through experimental methods, and subsequently propose a novel equivalent circuit based on the obtained results.

Nowadays, various methods can be used to replace a real induction motor with alternative circuits. Those methods can be found in references [36]–[38]. Those methods gathered on the Figure 1.

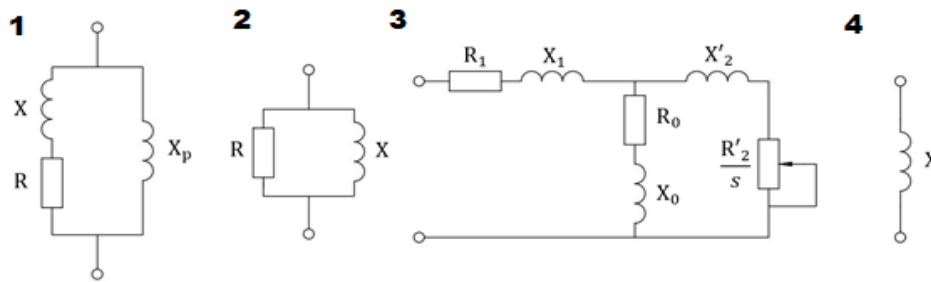


Figure 1. Equivalent circuits of an asynchronous motor at higher harmonics

Let's consider each scheme separately. Scheme 1 is proposed for compiling a load equivalent circuit and calculating modes with higher harmonics in the council on large electric systems (CIGRE) publication [20]. The formulas that are offered for each element of the scheme are as:

$$X_p = j \frac{nR}{6.7 \left( \frac{Q_{nom}}{P_{nom}} \right)^{-0.74}} \quad (1)$$

$$X = j0.073nR, \quad (2)$$

$$R = \frac{U^2}{P_{nom}} \quad (3)$$

probably, such an equivalent circuit is presented for a generalized electrical load and raises questions about the use of empirical coefficients in the formula. In addition, the frequency response of active resistance is assumed to be unchanged in this equivalent circuit.

In scheme 2, the conventional equivalent circuit for an asynchronous electric motor is depicted, in which the reactance is proportional to the order of the harmonic components and the active resistance is independent of frequency. Additionally, in a parallel connection, as the order of the harmonic increases, the current will flow more freely through the branch with active resistance, while the branch with inductive resistance will have less impact at higher harmonics. It also also takes note of the conventional equivalent circuit, which consists of a series connection of active and inductive resistances, and in which the parameters depend on how consistently the circuit's current flows [20].

$$R = \frac{U^2}{P_{nom}}, \quad (4)$$

$$X = j \frac{U^2 n}{Q_{nom}}. \quad (5)$$

A more detailed equivalent circuit (circuit 3) of an induction motor is given in [34], [35]. This circuit is called a single-phase equivalent circuit of an asynchronous motor. The magnetizing circuit is not taken into account in this calculation. The impedance is calculated using the (6) and (7):

$$X_{mn} = jn \cdot (X_1 + X'_2). \quad (6)$$

$$R_{mn} = (R_1 + R'_2) \left[ a\sqrt{n} + \frac{\pm n \cdot b \sqrt{\pm n - 1}}{\pm n - 1} \right], \quad (7)$$

where  $X_1$ ,  $X'_2$  и  $R_B$  short circuit resistances of the motor (the rotor is stationary). Coefficients a and b are recommended to be taken as 0.45 and 0.55, respectively. Active resistance has a change in proportion to the root of the harmonic number due to the effect of the skin effect. In the idling test for “AIR” motors, the motor parameters are listed in reference books but are not provided by manufacturers. Additionally, this formula work when the motor is operating in short circuit mode rather than the normal mode. This leads to significant mistakes in the substitution strategy.

Scheme 4 is considered in [37]. This equivalent circuit does not take into account the active resistance at the fundamental and higher harmonic frequencies. The authors note that such resistance can be neglected and this leads to an insignificant error in the calculations of regimes with higher harmonics. However, in some cases, not taking into account active resistance can lead to more significant errors, for example, when calculating modes with capacitor units. Also, the reactance at higher harmonics changes in proportion to the resistance at the fundamental frequency, taking into account the multiplicity of the starting current.

$$Z_n = X_n = n \frac{U_\phi}{k_n I_\phi}. \quad (8)$$

Various empirical coefficients are also present in the works [39], [40]. However, due to the fact that the methods of using these schemes are not analyzed in detail by the authors for the understanding of other readers, they were not considered. Thus, there is a significant variety of equivalent circuits for asynchronous electric motors when calculating modes with higher harmonics. In this work, the task was set to evaluate and compare the existing equivalent circuits of an asynchronous motor at higher harmonics using simulation modeling and experimental studies in the laboratory.

## 2. METHOD

To solve the problem, 2 methods were used: simulation and the laboratory experiment. Simulation was executed via MATLAB Simulink, SimPowerSystems library was used. Simulation is described in sub-section 2.1. Description of a laboratory experiment given in sub-section 2.2.

### 2.1. Simulation via MATLAB Simulink

In this work, a simulation model (SM) for research was developed, which is shown in Figure 2. The parameters for the induction motor block were calculated using the parameter estimator function from the nominal parameters. The load for the motor was modeled by a stepwise torque surge. In total, 4 experiments were carried out with a load of 25, 50, 75, and 100% of the nominal torque.

Oscillograms were recorded from a digital oscilloscope and then the voltages and currents were expanded into a fourier series using fast fourier transformation (FFT) analysis. The resistance amplitude at the nth harmonic was determined by dividing the phase voltage amplitude by the phase current amplitude:

$$Z_n = \frac{U_n}{I_n} \quad (9)$$

the resistances for the series circuit were calculated by multiplying by the sine and cosine of the phase difference of the voltage and current harmonics.

$$R_n = Z_n \cdot \cos\varphi_n \quad (10)$$

$$X_n = Z_n \cdot \sin\varphi_n \quad (11)$$

Thus, the graphs for the series harmonic equivalent circuit were obtained: n=1, 5, 7, 11, 13 in the simulation with a 6-pulse rectifier. The border value 13 was chosen to make a comparison of the simulation with experiment, since the contribution of higher harmonics to the total current decreased with harmonic number, which reduces measurement accuracy. The plots were gathered and put on the figures that are analysed and discussed in sub-section 3.1.

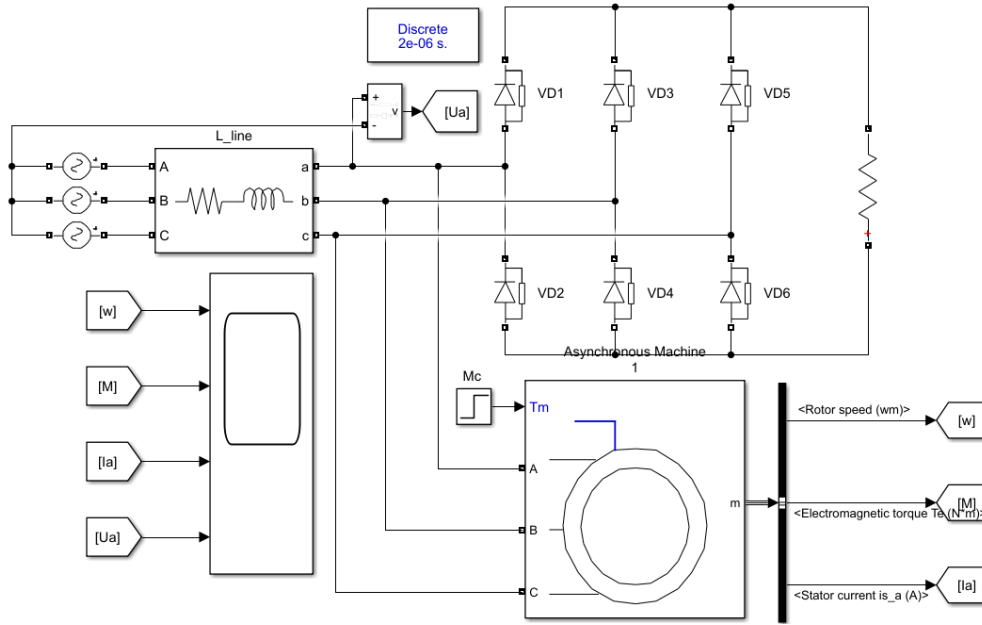


Figure 2. Simulation model with six-pulse rectifier

## 2.2. Experimental studies

The general scheme of the laboratory bench on which the experiment was carried out is shown in Figure 3. Where M is an asynchronous motor of the 4A90L6UZ or 4A100L2UZ series. Thyristor rectifier (TR) is a 6-pulse bridge thyristor rectifier, thyristor power controller (TPC) is a TRM-3M-30 thyristor power controller,  $X_L$  is an inductor with  $L=3.7$  mH,  $R_L=0.7$  Ohm, U is a three-phase voltage source with 220 V root mean square (RMS) value.

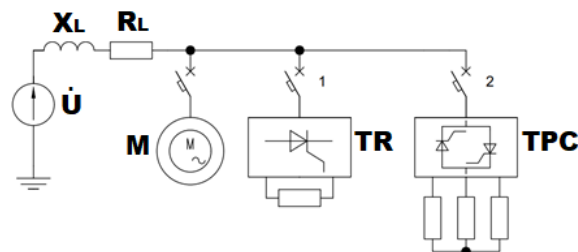


Figure 3. Electrical diagram of the laboratory bench

In laboratory conditions, two motors of different power were used. The nominal parameters of the motors are given in Table 1. A direct current (DC) motor with independent excitation was used as a load on the shaft of the asynchronous motor. The shaft power for the two motors was changed in steps. For a 1.5 kW motor, the powers were as follows: P1-188.76 W; P2-373.92 W; P3-512.08 W; P4-613.44 W load steps. For a 5.5 kW motor shaft power: P1-0 W, P2-910 W, P3-1650 W. The maximum values of the load steps of asynchronous motors were selected based on current limitations in laboratory conditions.

To generate higher harmonic currents in the motor power supply network, a six-pulse thyristor rectifier assembled according to the Larionov scheme was used with a 1.5 kW tubular electric heater connected to it and a TRM-3M-30 thyristor power controller connected in anti-parallel circuit, with tubular heaters connected in three phases. Thus, a 6-pulse thyristor rectifier generates harmonics with numbers  $6n \pm 1$ , and a thyristor power controller generates  $3n \pm 1$ , where  $n=1, 2, 3, \dots$  is a natural series. The voltage for consumers was distorted due to the presence of an active-inductive character in the resistance line. Network frequency-50 Hz.

To capture the instantaneous values of phase voltages and phase a current, a digital oscilloscope with a sampling frequency of 1,000 points per period was used. The resulting data in the csv-file format was then

uploaded and processed in MATLAB. The method for calculating the resistances coincides with the method for simulation modeling described above.

In the first experiment, an asynchronous motor and a 6-pulse thyristor rectifier were switched on in parallel at different loads on the motor. Thus, graphs were obtained for a series equivalent circuit on harmonics:  $n = 1, 5, 7, 11, 13$ . To increase the number of points on the plot, a second experiment was carried out.

In the second experiment, a thyristor power controller was switched on in parallel with the motor, but the resistances were obtained for harmonics with serial numbers  $n=1, 2, 4$ . The same experiments were carried out with a 5.5 kW motor. The plots were gathered and put on the figures that are analysed and discussed in sub-section 3.2.

Table 1. Parameters of induction motors 4A90L6UZ and 4A100L2UZ

Motor	4A90L6UZ	4A100L2UZ
Pnom (kW)	1.5	5.5
$\omega$ (rpm)	920	2,900
Inom (A)	7.00/4.05	19.13/11.07
Unom (V)	220/380	220/380
$\eta$ (%)	76	85.7
$\cos\phi$	0.75	0.88
Ist/Inom	5.5	7.5
Tst/Tnom	2	2.2
Tmax/Tnom	2.1	2.3
Tnom (N·m)	15.57	18.11
J (kg·m <sup>2</sup> )	0.0066	0.008

### 3. RESULTS AND DISCUSSION

#### 3.1. Simulation results

At given loads, which were: 25%, 50%, 75%, and 100% of nominal load, as a result of simulation modeling, dependences were obtained in the form of graphs of active and reactive resistances of motors on the number of harmonics. The resulting graphs were connected together on Figure 4 for 1.5 kW AM and on Figure 5 for 5.5 kW AM to evaluate how the load on the motor affects the impedance at higher harmonics. You may see it on Figure 4(a) for resistance, Figure 4(b) for reactance for 1.5 kW AM and on Figure 5(a) for resistance, Figure 5(b) for reactance for 5.5 kW AM.

According to the graphs obtained during simulation below, it can be seen that:

- Active resistance has a constant value at higher harmonics. Most likely, this is due to the fact that the standard MATLAB Simulink induction motor block does not take into account the skin effect, which manifests itself in the fact that the resistance on the higher harmonic's changes in proportion to the square root of the harmonic number.
- The reactance changes in direct proportion to the harmonic number. The resistance of the first harmonic and the resistance of higher harmonics lies on different lines.
- Active and reactive resistances at higher harmonics do not depend on the motor load.

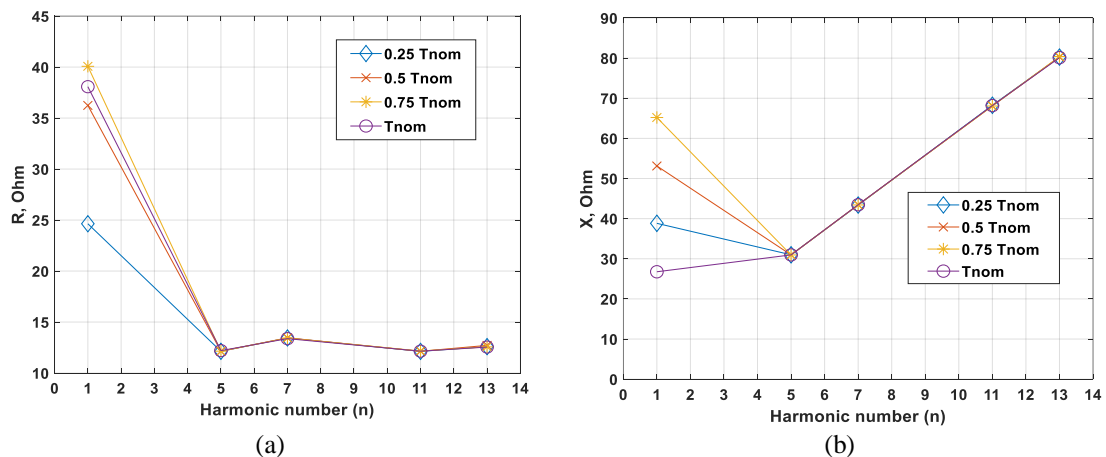


Figure 4. Impedance of 1.5 kW motor at various loads, studied through the use of simulation (a) resistance and (b) reactance

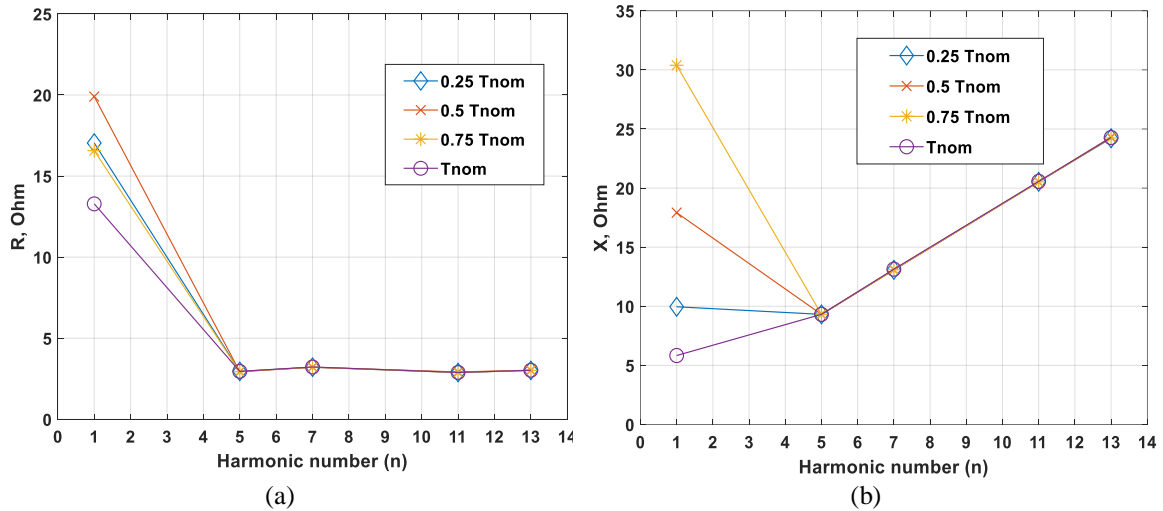


Figure 5. Impedance of 5.5 kW motor at various loads, studied through the use of simulation (a) resistance and (b) reactance

3.2. Experiment results

At given loads, as a result of a laboratory experiment, dependencies were obtained in the form of graphs of active and reactive resistances of motors on the number of harmonics: Figure 6 and Figure 7 respectively for 1.5 kW AM and 5.5 kW AM. The SCR-silicon controlled rectifier index indicates that the harmonics were generated by the thyristor regulator. The source of the remaining harmonics was a thyristor rectifier. Subfigures represent the results of a laboratory experiment. Figure 6(a) for resistance, Figure 6(b) for reactance for 1.5 kW AM and on Figure 7(a) for resistance, Figure 7(b) for reactance for 5.5 kW AM. According to the graphs obtained in laboratory modeling below, the following conclusions can be drawn:

- Active resistance at higher harmonics increases with increasing frequency of the supply voltage, which is due to the skin effect.
- The reactance at higher harmonics changes in direct proportion to the harmonic number.
- The value of resistance at higher harmonics do not depend on the load of the electric motor and the type of source of higher harmonics that creates distortions in the mains voltage.

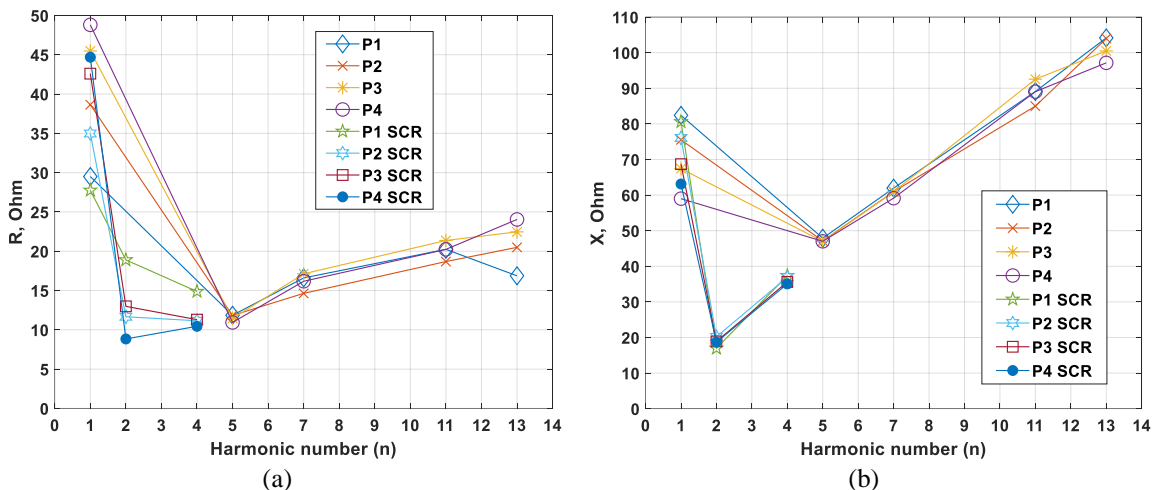


Figure 6. Impedance of 1.5 kW motor at various loads with various harmonic sources, studied through the use of experiment (a) resistance and (b) reactance

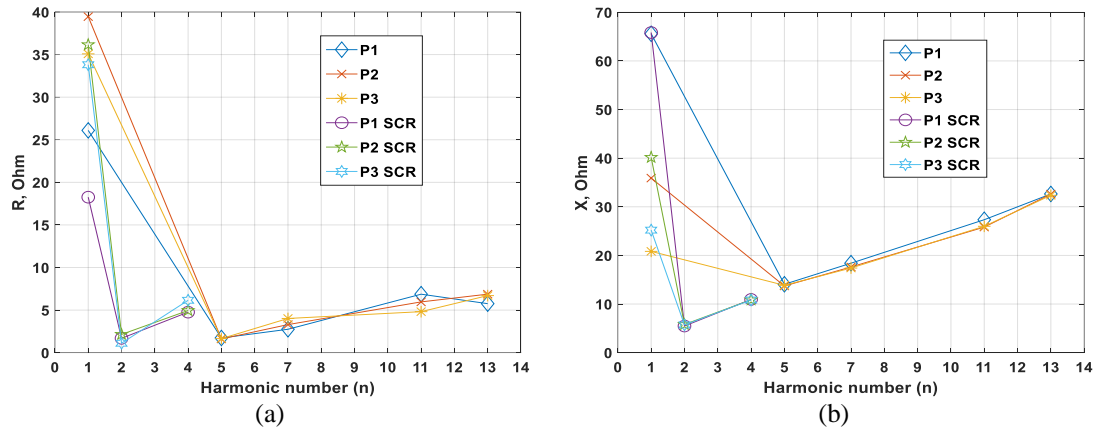


Figure 7. Impedance of 5.5 kW motor at various loads with various harmonic sources, studied through the use of simulation (a) resistance and (b) reactance

3.3. Comparative analysis

As a result of the transformation of the formula for calculating the impedance of AM at higher harmonics to a series connection, the data were obtained, which are presented in Table 2 for a 1.5 kW motor and Table 3 for a 5.5 kW motor. It is assumed that the impedance is calculated at the nominal load mode, but it was previously found that the load mode does not affect the resistance and reactance on higher harmonics. The reference values for “AIR” motors used in the third method were taken from [41].

Table 2. The 1.5 kW induction motor resistances and reactances obtained by various methods

n	R (Ohm)						X (Ohm)					
	1	2	3	4	Im.m	Exp	1	2	3	4	Im.m	Exp
1	1.13	18.15	-	-	-	4.89	5.94	16.01	0.23	5.71	-	9.40
2	3.76	27.01	0.74	-	-	6.92	10.48	11.91	0.46	11.43	-	18.80
4	9.05	30.77	0.74	-	-	9.79	15.33	6.78	0.92	22.86	-	37.60
5	10.88	31.29	0.79	-	12.2	10.94	16.72	5.52	1.15	28.57	30.97	47.00
7	13.21	31.76	0.88	-	13.4	12.95	19.05	4.00	1.61	40.00	43.46	65.80
11	15.24	32.06	1.05	-	12.1	16.23	24.01	2.57	2.53	62.86	68.17	103.40
13	15.70	32.12	1.13	-	12.5	17.64	26.76	2.18	2.99	74.29	80.12	122.20

Table 3. The 5.5 kW induction motor resistances and reactances obtained by various methods

n	R (Ohm)						X (Ohm)					
	1	2	3	4	Im.m	Exp	1	2	3	4	Im.m	Exp
1	0.90	8.73	-	-	-	0.74	2.68	0.76	0.10	5.71	-	2.77
2	2.49	8.78	0.32	-	-	1.04	4.02	0.38	0.20	11.43	-	5.54
4	4.44	8.80	0.32	-	-	1.48	4.76	0.19	0.40	22.86	-	11.08
5	4.90	8.80	0.34	-	2.96	1.65	4.99	0.15	0.50	28.57	9.32	13.85
7	5.39	8.80	0.38	-	3.23	1.95	5.55	0.11	0.70	40.00	13.14	19.39
11	5.74	8.80	0.45	-	2.89	2.45	7.08	0.07	1.10	62.86	20.57	30.46
13	5.82	8.80	0.48	-	3.02	2.66	7.97	0.06	1.30	74.29	24.28	36.00

For clarity, the data from the tables is presented in the graphs on the Figures 8 and 9: impedances of 1.5 kW and 5.5 kW Figure 8 and Figure 9 respectively. Subfigures contain the comparative graphs of motor representation when the parts of the impedance: resistance and reactance are connected in series. Figure 8(a) for resistance, Figure 8(b) for reactance for 1.5 kW AM and on the Figure 9(a) for resistance, Figure 9(b) for reactance for 5.5 kW AM. Here Im.m are the values obtained during simulation; Exp-values obtained from laboratory simulation, U/I-point of resistance or reactance calculated according to nominal parameters to see the pattern of this point the impedance at the first harmonic in the nominal mode at higher harmonics. The number 1, 2, 3, 4 display the values that were calculated with different methods presented on Figure 1.

Comparing the equivalent circuits presented in the first section with experimental data and simulation modeling see Figure 8 and Figure 9, we can draw the following conclusions:

- When calculating the active resistance at higher harmonics, the closest values to the experimental data are obtained based on the use of the equivalent circuit in method 1 and simulation. With an increase in the power of the AM, the calculation error based on method 1 increases.

- When calculating the reactance, the absolute error increases in proportion to the harmonic number, since the experimental values have a directly proportional dependence, and for equivalent circuits with a linear dependence, the relative error remains constant. The closest values to the experimental data are obtained on the basis of simulation modeling. It should be noted that the error in calculating the resistance at higher harmonics depends on the calculated value of the resistance at the fundamental frequency.

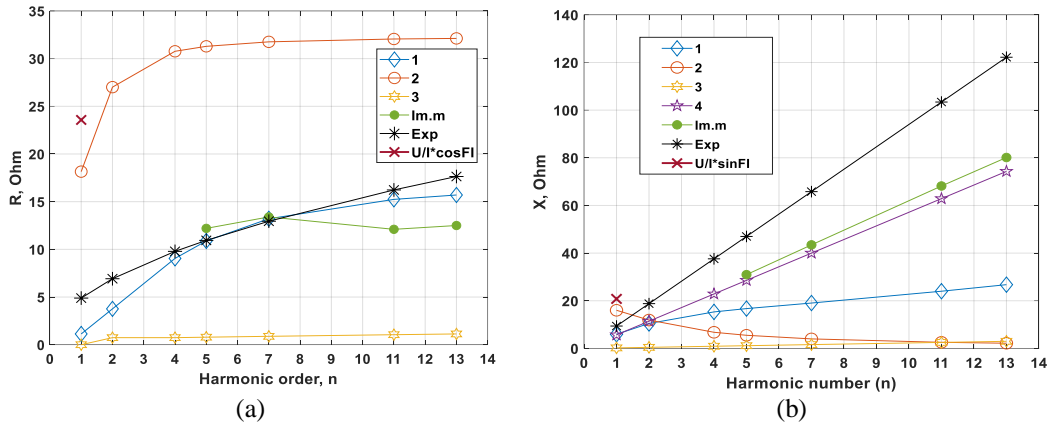


Figure 8. Comparative graphs of various methods of 1.5 kW induction motor representation on higher harmonics and experimentally obtained data on its nominal power (a) resistances and (b) reactances

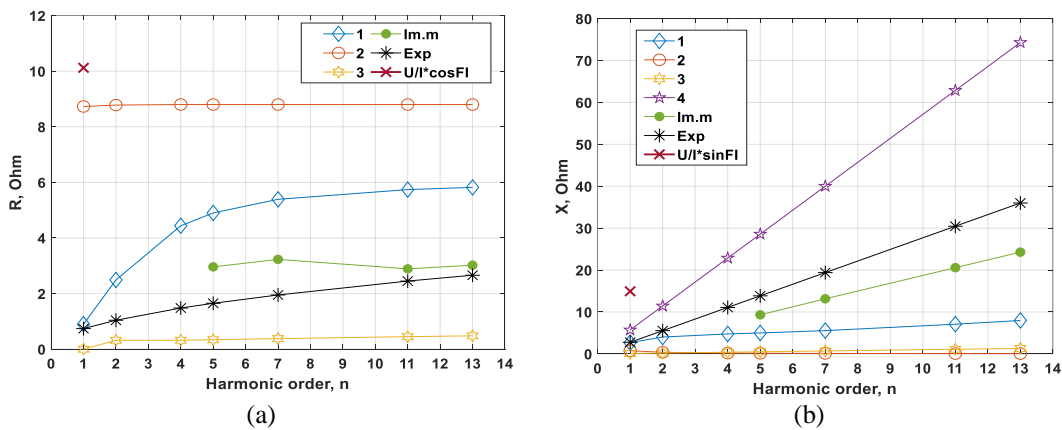


Figure 9. Comparative graphs of various methods of 5.5 kW induction motor representation on higher harmonics and experimentally obtained data on its nominal power (a) resistances and (b) reactances

Thus, when calculating modes with higher harmonics based on simplified SM equivalent circuits, an additional error arises. Simulation modeling shows the closest results with respect to experimental data. However, it is often necessary to carry out an estimated calculation based on simplified equivalent circuits. Based on this study, the closest results to the experimental ones were shown by equivalent circuits based on method 1 for active resistance and method 4 for inductive resistance.

As part of further research, it is proposed to calculate the resistance of higher harmonics according to the formula from the motor passport data, since they are always given in the reference book, or on the nameplate:

$$R_n = k_R \frac{U_{HOM}}{I_{HOM}} \cos\varphi \cdot \sqrt{n}, \tag{12}$$

$$X_n = k_X \frac{U_{HOM}}{I_{HOM}} \sin\varphi \cdot n, \tag{13}$$

where k is the reduction factor for the resistance of the first harmonic to calculate higher harmonics. The value of these coefficients may vary depending on the motor. For a 1.5 kW motor, the coefficients  $k_R$  and  $k_X$  were



0.207 and 0.452, respectively. For a 5.5 kW motor, the coefficients  $k_R$  and  $k_X$  were 0.073 and 0.185, respectively. Since only 2 motors were used in this work, it was impossible to find the dependence of  $k$  on the parameters of various motors, for example, power. With the help of simulation modeling, this dependence cannot be found, since the values of the experiment and simulation differ greatly. The study of this dependence is the goal of future work.

#### 4. CONCLUSION

The paper presents an analysis of the equivalent circuits of an asynchronous motor namely a squirrel-cage rotor, which is necessary when performing calculations in the presence of distortions in the supply voltage. The resistance values at higher harmonics of an induction motor are obtained on the basis of experimental studies in laboratory conditions. The results of the experimental data were compared with the results of simulation modeling and existing methods for calculating resistances at higher harmonics. Methods have been identified that show the closest results in comparison with experimental data. It is also determined that the resistance at higher harmonics does not depend on the operating mode of the asynchronous motor, and the load on the shaft determines only the resistance at the fundamental harmonic. This makes it possible to calculate the resistance at higher harmonics based only on the value of the resistance at the fundamental frequency. It is proposed to represent the equivalent circuit of asynchronous motor on the basis of a sequential circuit.

#### ACKNOWLEDGEMENTS

This research was financially supported by the Russian Science Foundation Grant No. 21-79-10027, <https://rscf.ru/en/project/21-79-10027>.




#### REFERENCES

- [1] J. M. Munoz-Guijosa, S. B. Krylctov, and S. V. Solovev, "Application of an active rectifier used to mitigate currents distortion in 6-10 KV distribution grids," *Journal of Mining Institute*, vol. 236, no. 2, pp. 229–238, Apr. 2019, doi: 10.31897/PMI.2019.2.229.
- [2] C. Venugopal, T. Bhuvanawari, and S. Immanuel, "Analysis of 12 pulse three-phase to three-phase cycloconverter drive for induction motor load," *Journal of Engineering Research*, vol. 11, no. 1, p. 100018, Mar. 2023, doi: 10.1016/j.jer.2023.100018.
- [3] L. R. L. V. Raj, A. Jidin, K. A. Karim, T. Sutikno, R. Sundram, and M. H. Jopri, "Improved torque control performance of direct torque control for 5-phase induction machine," *International Journal of Power Electronics and Drive Systems (IJPEDS)*, vol. 3, no. 4, pp. 391–399, Dec. 2013, doi: 10.11591/ijpeds.v3i4.5249.
- [4] I. C. Barutcu, E. Karatepe, and M. Boztepe, "Impact of harmonic limits on PV penetration levels in unbalanced distribution networks considering load and irradiance uncertainty," *International Journal of Electrical Power & Energy Systems (IJPES)*, vol. 118, p. 105780, Jun. 2020, doi: 10.1016/j.ijepes.2019.105780.
- [5] R. R. A. Fortes, R. F. Buzo, and L. C. O. De-Oliveira, "Harmonic distortion assessment in power distribution networks considering DC component injection from PV inverters," *Electric Power Systems Research*, vol. 188, p. 106521, Nov. 2020, doi: 10.1016/j.epsr.2020.106521.
- [6] A. Menti, D. Barkas, S. Kaminaris, and C. S. Psomopoulos, "Supraharmonic emission from a three-phase PV system connected to the LV grid," *Energy Reports*, vol. 7, pp. 527–542, Nov. 2021, doi: 10.1016/j.egy.2021.07.100.
- [7] A. Belsky, V. S. Dobush, and S. F. Haikal, "Operation of a single-phase autonomous inverter as a part of a low-power wind complex," *Journal of Mining Institute*, vol. 239, no. 5, pp. 564–569, Oct. 2019, doi: 10.31897/PMI.2019.5.564.
- [8] A. Mishra and K. Chatterjee, "Harmonic analysis and attenuation using LCL-filter in doubly fed induction generator based wind conversion system using real time simulation based OPAL-RT," *Alexandria Engineering Journal*, vol. 61, no. 5, pp. 3773–3792, May 2022, doi: 10.1016/j.aej.2021.08.079.
- [9] M. Bašić, D. Vukadinović, I. Grgić, and M. Bubalo, "Energy efficient control of a stand-alone wind energy conversion system with AC current harmonics compensation," *Control Engineering Practice*, vol. 93, p. 104185, Dec. 2019, doi: 10.1016/j.conengprac.2019.104185.
- [10] N. H. A. Kahar, A. F. Zobia, R. A. Turkey, A. M. Zobia, S. H. E. A. Aleem, and B. Ismail, "Comparative analysis of optimal damped and undamped passive filters using MIDACO-solver," *Ain Shams Engineering Journal*, vol. 14, no. 8, p. 102056, Aug. 2023, doi: 10.1016/j.asej.2022.102056.
- [11] K. Kritsanawan, U. Leeton, and T. Kulworawanichpong, "Harmonic mitigation of AC electric railway power feeding system by using single-tuned passive filters," *Energy Reports*, vol. 8, pp. 1116–1124, Nov. 2022, doi: 10.1016/j.egy.2022.05.276.
- [12] I. D. Melo, J. L. R. Pereira, A. M. Variz, and P. F. Ribeiro, "Allocation and sizing of single tuned passive filters in three-phase distribution systems for power quality improvement," *Electric Power Systems Research*, vol. 180, p. 106128, Mar. 2020, doi: 10.1016/j.epsr.2019.106128.
- [13] D. Chen, Z. Lin, L. Xiao, W. Yan, and Y. Guo, "An inductor design method based on multi-objective optimized algorithm for LCL-type shunt active power filter," *Energy Reports*, vol. 8, pp. 502–511, Nov. 2022, doi: 10.1016/j.egy.2022.09.157.
- [14] A. K. Dubey, J. P. Mishra, and A. Kumar, "Comparative analysis of ROGI based shunt active power filter under current fed and voltage fed type non-linear loading condition," *IFAC-PapersOnLine*, vol. 55, no. 1, pp. 156–161, 2022, doi: 10.1016/j.ifacol.2022.04.026.
- [15] Y. Abouelmahjoub *et al.*, "Advanced control and observation of shunt active power filter connected to PV system," *IFAC-PapersOnLine*, vol. 55, no. 12, pp. 31–36, 2022, doi: 10.1016/j.ifacol.2022.07.284.
- [16] H. Eroğlu, E. Cuce, P. M. Cuce, F. Gul, and A. Iskenderoğlu, "Harmonic problems in renewable and sustainable energy systems: A comprehensive review," *Sustainable Energy Technologies and Assessments*, vol. 48, p. 101566, Dec. 2021, doi: 10.1016/j.seta.2021.101566.




- [17] K. Jha and A. G. Shaik, "A comprehensive review of power quality mitigation in the scenario of solar PV integration into utility grid," *e-Prime - Advances in Electrical Engineering, Electronics and Energy*, vol. 3, p. 100103, Mar. 2023, doi: 10.1016/j.prime.2022.100103.
- [18] K. Kularbphetpong and C. Boonseng, "HPFs filtering solutions for reduced the harmonic current generated by SMPS and ac drive systems," *Energy Reports*, vol. 6, pp. 648–658, Feb. 2020, doi: 10.1016/j.egy.2019.11.133.
- [19] H. Alenius, R. Luhtala, and T. Roinila, "Amplitude design of perturbation signal in frequency-domain analysis of grid-connected systems," *IFAC-PapersOnLine*, vol. 53, no. 2, pp. 13161–13166, 2020, doi: 10.1016/j.ifacol.2020.12.123.
- [20] C.I.G.R.E, "Network modelling for harmonic studies," *CIGRE*, vol. 33, p. 241, 2019.
- [21] M. H. Jopri, M. R. Ab Ghani, A. R. Abdullah, T. Sutikno, M. Manap, and J. Too, "Naïve bayes and linear discriminate analysis based diagnostic analytic of harmonic source identification," *Indonesian Journal of Electrical Engineering and Computer Science (IJECS)*, vol. 20, no. 3, pp. 1626–1633, Dec. 2020, doi: 10.11591/ijeecs.v20.i3.pp1626-1633.
- [22] E. Karami, E. Hajipour, M. Vakilian, and K. Rouzbehi, "Analysis of frequency-dependent network equivalents in dynamic harmonic domain," *Electric Power Systems Research*, vol. 193, p. 107037, Apr. 2021, doi: 10.1016/j.epr.2021.107037.
- [23] B. Gao, Y. Wang, and W. Xu, "An impedance matrix model of DFIG for harmonic power flow analysis considering DC-link dynamics," *International Journal of Electrical Power and Energy Systems (IJEPE)*, vol. 148, p. 108895, Jun. 2023, doi: 10.1016/j.ijepe.2022.108895.
- [24] Ö. C. Sakinci, A. Lekić, and J. Beerten, "Generalized impedance-based AC/DC power system modeling for harmonic stability analysis," *International Journal of Electrical Power and Energy Systems (IJEPE)*, vol. 143, p. 108456, Dec. 2022, doi: 10.1016/j.ijepe.2022.108456.
- [25] S. Simon, A. Winkens, A. Monti, and A. Ulbig, "Extraction of frequency-dependent impedances of residential loads in low-voltage grids for harmonic stability assessment," *Electric Power Systems Research*, vol. 212, p. 108528, Nov. 2022, doi: 10.1016/j.epr.2022.108528.
- [26] Y. Zhang *et al.*, "Equivalent modeling method of induction motor contribution to short-circuit current," *Energy Reports*, vol. 8, pp. 1202–1210, Nov. 2022, doi: 10.1016/j.egy.2022.08.102.
- [27] V. Z. Castillo, H. S. de Boer, R. M. Muñoz, D. E. H. J. Gernaat, R. Benders, and D. Van Vuuren, "Future global electricity demand load curves," *Energy*, vol. 258, p. 124741, Nov. 2022, doi: 10.1016/j.energy.2022.124741.
- [28] M. Y. Shabalov, Y. L. Zhukovskiy, A. D. Buldysko, B. Gil, and V. V. Starshaia, "The influence of technological changes in energy efficiency on the infrastructure deterioration in the energy sector," *Energy Reports*, vol. 7, pp. 2664–2680, Nov. 2021, doi: 10.1016/j.egy.2021.05.001.
- [29] S. A. B. Santos, J. M. Soares, G. C. Barroso, and B. Athayde-Prata, "Demand response application in industrial scenarios: a systematic mapping of practical implementation," *Expert Systems with Applications*, vol. 215, p. 119393, Apr. 2023, doi: 10.1016/j.eswa.2022.119393.
- [30] N. D. Senchilo and D. A. Ustinov, "Method for determining the optimal capacity of energy storage systems with a long-term forecast of power consumption," *Energies*, vol. 14, no. 21, p. 7098, Oct. 2021, doi: 10.3390/en14217098.
- [31] K. K. Jaiswal *et al.*, "Renewable and sustainable clean energy development and impact on social, economic, and environmental health," *Energy Nexus*, vol. 7, p. 100118, Sep. 2022, doi: 10.1016/j.nexus.2022.100118.
- [32] Y. Zhukovskiy, P. Tsvetkov, A. Buldysko, Y. Malkova, A. Stoianova, and A. Koshenkova, "Scenario modeling of sustainable development of energy supply in the arctic," *Resources*, vol. 10, no. 12, p. 124, Dec. 2021, doi: 10.3390/resources10120124.
- [33] P. Tsvetkov, "Climate policy imbalance in the energy sector: time to focus on the value of CO2 utilization," *Energies*, vol. 14, no. 2, p. 411, Jan. 2021, doi: 10.3390/en14020411.
- [34] M. Bailera, P. Lisbona, B. Peña, and L. M. Romeo, "A review on CO2 mitigation in the iron and steel industry through power to x processes," *Journal of CO2 Utilization*, vol. 46, p. 101456, Apr. 2021, doi: 10.1016/j.jcou.2021.101456.
- [35] F. Nocito and A. Dibenedetto, "Atmospheric CO2 mitigation technologies: carbon capture utilization and storage," *Current Opinion in Green and Sustainable Chemistry*, vol. 21, pp. 34–43, Feb. 2020, doi: 10.1016/j.cogsc.2019.10.002.
- [36] J. Arrillaga, B. C. Smith, N. R. Watson, and A. R. Wood, *Power System Harmonic Analysis*. John Wiley and Sons, 1997.
- [37] I. V. Zhezhelenko, "Higher harmonics in power supply systems of an industrial enterprise," *and additional M.: Energotomizdat*, p. 331, 2006.
- [38] L. R. L. V. Raj, A. Jidin, C. W. M. F. C. W. M. Zalani, K. A. Karim, G. W. Yen, and M. H. Jopri, "Improved performance of DTC of five-phase induction machines," in *Proceedings of the 2013 IEEE 7th International Power Engineering and Optimization Conference, PEOCO 2013*, Jun. 2013, pp. 613–618, doi: 10.1109/PEOCO.2013.6564621.
- [39] S. S. Smirnov, *Higher harmonics in high voltage networks*. Novosibirsk: Nauka, 2010.
- [40] O.T. Geraskin, V.V. Cherepanov, *Application of computer technology for the calculation of higher harmonics in electrical networks*. Moscow: VIPKenergo, 1987.
- [41] A. E. Kravchik, M. M. Schlaf, V. I. Afonin, and E. A. Sobolenskaya, *Series 4A asynchronous motors*. Handbook, M: Energoizdat, 1982.

## BIOGRAPHIES OF AUTHORS






**Aleksandr Skamyin**    was born in Volkhov, Russia on 1986. He received his B.Eng. and Ph.D. degree in electrical engineering from Saint-Petersburg Mining University (Russian Federation) in 2007 and 2011, respectively. From 2011 till 2015 he was the assistant in National Mineral Resources University (Mining University), Saint-Petersburg, Russian Federation. Since 2015, he is an associated professor in Saint-Petersburg Mining University (Russian Federation). His research interests include power quality, reactive power compensation in the presence of harmonics, and regulation of power consumption mode. He can be contacted at email: skamin\_an@pers.spmi.ru.






**Yaroslav Shklyarskiy**    is a Lecturer in General Electrical Engineering Department at the Saint-Petersburg Mining University. He received a habilitated Doctor of Technical Sciences degree from the Krakow Mining and Metallurgical Academy in 1991. He received his Ph.D. degree (doctoral dissertation) in Electrical Engineering from Saint-Petersburg Mining University in 2004. He has been lecturing at the Saint-Petersburg Mining University since 1977. From 2004 and till now he is academic supervisor of postgraduate students. He is currently an editorial board member of the Electrical Power Quality and Utilization Journal and Journal of Mining Institute. His research interests include the field of power quality, reactive power compensation, power flow control, and regulation. He can be contacted at email: js-10@mail.ru.






**Kirill Lobko**    is a postgraduate student of St. Petersburg Mining University with a degree in Mining Automation and Electrification. During his studies as an engineer, he took internships in the Belarusian National Technical University in Minsk, Belarus. At the moment he works in the field of electrical engineering focused on the improving the efficiency of the electrical network in the presence of higher harmonics. He can be contacted at email: kirill1999lobko@yandex.ru.






**Vasily Dobush**    was born in Uchkulach, Uzbekistan in 1988. He received his B.Eng. and Ph.D. degree in electrical engineering from Saint-Petersburg Mining University (Russian Federation) in 2010 and 2013, respectively. From 2013 till 2017 he was assistant in National Mineral resources University (Mining University), Saint-Petersburg, Russian Federation. Since 2017, he is associated professor in Saint-Petersburg Mining University (Russian Federation). His research interests include power quality, power harmonics, active harmonic filters, and power converters. He can be contacted at email: dobush\_vs@pers.spmi.ru.



**Tole Sutikno**    received B.Eng. and M.Eng. in electrical engineering from Universitas Diponegoro and Universitas Gajah Mada, Indonesia, in 1999 and 2004, respectively, and the Ph.D. degree from Universiti Teknologi Malaysia in 2016. He is an Associate Professor with the Electrical Engineering Department, Universitas Ahmad Dahlan, and the leader of Embedded Systems and Power Electronics Research Group (ESPERG). He has published hundreds of research results in the form of scientific articles published in reputable international journals, international proceedings, and books. In addition, he is active as an editor in several reputable international journals in the fields of electrical, computer and informatics engineering. His research interests include power electronics and electric motor control, industrial electronics and informatics, embedded systems, and the internet of things (IoT), renewable energy and electrical energy storage systems, and digital control systems (control, robotics and sensors). He can be contacted at email: tole@ee.uad.ac.id.



**Mohd Hatta Jopri**    received his B.Eng. from Universiti Teknologi Malaysia (UTM), Msc. in Electrical Power Engineering from Rheinisch-Westfälische Technische Hochschule Aachen (RWTH), Germany, and Ph.D. degree from Universiti Teknikal Malaysia Melaka (UTeM), respectively. Since 2005, he is an academia and research staff at UTeM. He is registered with Malaysia Board of Technologist (MBOT), Board of Engineers Malaysia (BEM) and a member of International Association of Engineers (IAENG). His research interests include power electronics and drive, power quality analysis, signal processing, machine learning, and data science. He can be contacted at email: hatta@utem.edu.my.